

# Dilepton emission as a novel probe of QCD critical point

Gaoqing Cao,<sup>1,\*</sup> Xiaofeng Luo,<sup>2,†</sup> and Wei-jie Fu<sup>3,‡</sup>

<sup>1</sup>*School of Physics and Astronomy, Sun Yat-sen University, Zhuhai 519088, China*  
<sup>2</sup>*Key Laboratory of Quark & Lepton Physics (MOE) and Institute of Particle Physics,  
Central China Normal University, Wuhan 430079, China*

<sup>3</sup>*School of Physics, Dalian University of Technology, Dalian, 116024, China*  
(Dated: January 1, 2026)

In this work, we propose dilepton emission rate (DER) as a sensitive probe of QCD critical point based on the extended Polyakov-quark-meson model. The model could successfully capture two main mechanisms for dilepton production,  $\pi^\pm$  and quark-antiquark annihilations on one hand, and self-consistently account for chiral transition and (de-)confinement on the other hand. Along the chemical freezeout lines, all the moments of the DER peak show similar extremal features as those of light quark mass, thus the DER can well reflect the change of chiral symmetry and criticality. More importantly, the DER can be directly measured in heavy ion collisions: Compared to the baryon number fluctuations, the DER fluctuations are found to be more drastic in the critical region and more sensitive to the relative location of the critical point. However, recent statistics of DER in heavy ion collision is not large enough to perform event-by-event measurement, instead we propose to study the baseline subtracted DER: For a given dilepton center of mass, the largest deviation shows up around the point where the light quark mass fluctuation is the strongest.

*Introduction.* According to most recent Beam Energy Scan Phase-II at RHIC in USA [1–3], the QCD matter is in the hadronic phase for the collision energy  $\sqrt{S_{NN}} = 3 \text{ GeV}$  [1, 2] and the baryon number kurtosis shows no critical peak from  $\sqrt{S_{NN}} = 7.7 \text{ GeV}$  up [3]. It is a consensus that the search of QCD critical point is now at a “critical point”: whether or not a peak [4–7] would show up in between these collision energies could give a definite conclusion on whether or not the QCD critical point can be detected in relativistic heavy ion collisions (HICs). In a few years, several other low-energy facilities would join the search, such as the FAIR in Germany, NICA in Russia and HIAF in China, so it is now the best and most important period to explore the QCD criticality [8–11]. Especially, the illumination of lepton would be greatly improved in CBM experiment, it is essential to check possible leptonic signals for QCD critical point, such as dilepton emission rate (DER) [12, 13].

In principle, any observables sensitive to the QCD medium can serve as a probe of critical point, though the criterions might vary from one to another. Nevertheless, it is well known that the most significant feature of critical point is strong fluctuations nearby [14], so higher moments of the observables are always better choices since they are more sensitive to the fluctuations. How can one detect higher moments of the observables in HICs? Take the moments with respect to the chemical potential  $\mu_X$  ( $X$  is a conserved charge) for example, the expectation value of the observable  $\hat{O}$  is given in a grand canonical ensemble [15] by

$$\langle \hat{O} \rangle \equiv \frac{\text{Tr } \hat{O} e^{-\hat{H}/T + \hat{N}_X \mu_X / T}}{\text{Tr } e^{-\hat{H}/T + \hat{N}_X \mu_X / T}}, \quad (1)$$

and the  $n$ th order moments follow as

$$\begin{aligned} \frac{\partial \langle \hat{O} \rangle}{\partial (\mu_X / T)} &= \langle \delta \hat{O} \delta \hat{N}_X \rangle, \quad \frac{\partial^2 \langle \hat{O} \rangle}{\partial (\mu_X / T)^2} = \langle \delta \hat{O} (\delta \hat{N}_X)^2 \rangle, \\ \frac{\partial^3 \langle \hat{O} \rangle}{\partial (\mu_X / T)^3} &= \langle \delta \hat{O} (\delta \hat{N}_X)^3 \rangle - 3 \langle \delta \hat{O} \delta \hat{N}_X \rangle \langle (\delta \hat{N}_X)^2 \rangle, \dots \end{aligned} \quad (2)$$

with  $\delta \hat{O} \equiv \hat{O} - \langle \hat{O} \rangle$ . So, the higher moments of the observables are nothing but just the correlations between their fluctuations and higher order fluctuations of the total conserved charge,  $(\delta \hat{N}_X)^n$ . It is easy to extend that to mixed moments when several conserved charges are involved, such as  $X = B, Q, S$  in HICs [8, 9]. Usually, the moments with respect to  $\mu_B$  are the most sensitive for the search of QCD critical point in  $T - \mu_B$  plane [8, 9]. Regarding the dilepton emission rate  $\mathcal{R}$ , the correlation with baryon number fluctuations,  $\langle \delta \mathcal{R} (\delta \hat{N}_B)^n \rangle$ , should be measured event-by-event in HICs.

In this work, we propose that dilepton emission rate is a sensitive probe of QCD critical point. The Polyakov-quark-meson (PQM) model [16, 17] is extended by including vector sector [18] for the study, then the features of chiral transition and (de-)confinement could be transformed to those of dilepton emission. Along two realistic chemical freezeout lines [8], it is found that all the moments of the DER peak show similar extremal features as those of light quark mass, thus the DER can well reflect the change of chiral symmetry and help to locate the critical point. However, regarding the poor statistics in recent heavy ion collisions, the baseline subtracted DER can be regarded as an alternative probe.

*A chiral effective model.* Previously, the renormalizable 2 + 1 flavor Polyakov-quark-meson model [17] was successfully adopted to study the  $T - \mu_B$  phase diagram of QCD matter, and both the pseudocritical temperature and critical point were found to be consistent with

those from lattice QCD [19, 20] and functional QCD approaches [21–23]. So, it is convincible that the PQM model could well capture the QCD criticality and give useful hints on possible critical signals in heavy ion collisions. In Euclidean space with the metric  $g^{\mu\nu} = -\delta_{\mu\nu}$ , the original Lagrangian density of the PQM model [16] is given by

$$\begin{aligned} \mathcal{L}_{\text{PQM}}^0 = & \bar{\psi} \left[ i\gamma^\mu D_\mu - i\gamma^4 \frac{\mu_B}{3} - g_{\text{sq}} T^b (\sigma_b + i\gamma^5 \pi_b) \right] \psi \\ & + \frac{1}{2} [\partial_\mu \phi^{\dagger b} \partial^\mu \phi_b - m_\phi^2 \phi^{\dagger b} \phi_b] - h_1 [\text{Tr}(\phi^\dagger \phi)]^2 - h_2 \text{Tr}(\phi^\dagger \phi)^2 \\ & + \kappa [\text{Det}(\phi^\dagger) + \text{Det}(\phi)] + c_b \text{Tr} T^b (\phi^\dagger + \phi) - V(L), \end{aligned} \quad (3)$$

where  $\psi(x) = (u(x), d(x), s(x))^T$  denotes the three-flavor quark field with the charge matrix  $Q_q = \text{dia}(q_u, q_d, q_s)$ ,  $D_\mu = \partial_\mu + i Q_q A_\mu - ig_s \mathcal{A}^4$  is the covariant derivative with  $A_\mu$  the electromagnetic (EM) field and  $\mathcal{A}^4$  the temporal gluon field, and  $\phi \equiv T^b (\sigma_b + i\pi_b)$  is the scalar-pseudoscalar field matrix. To study the dilepton emission which is itself a direct QED effect, we choose  $\sigma_b + i\pi_b$  to be the eigenstates of electric charge with eigenvalues  $q_b$ . Correspondingly, the interaction matrices in flavor space are  $T^0 = \sqrt{\frac{1}{6}} \mathbf{1}$ ,  $T^{1,2} = \frac{\lambda^1 \mp i\lambda^2}{2\sqrt{2}}$ ,  $T^{4,5} = \frac{\lambda^4 \mp i\lambda^5}{2\sqrt{2}}$ ,  $T^b = \frac{\lambda^b}{2}$  ( $b = 3, 6, 7, 8$ ) with  $\lambda^b$  the Gell-Mann matrices [17]. In the physical vacuum,  $u$  and  $d$  quarks are almost degenerate and chiral symmetry is broken through the scalar channels, thus only the components  $b = 0, 8$  of  $c_b$  are supposed to be nonzero.

The Polyakov loop  $L \equiv \frac{1}{N_c} \text{Tr}_c e^{i g_s \int_0^{1/T} dx_4 \mathcal{A}^4}$  determines when the quark degrees of freedom are dynamically relevant in the QCD matter. For simplicity, we would set  $L = L^*$  even in the case with finite  $\mu_B$  and take the empirical expression for the pure gauge potential  $V(L)$  as given by Munich group [24],

$$\frac{V(L)}{T^4} = -\frac{a(T/T_0)}{2} L^2 - \frac{0.75}{3} L^3 + \frac{7.5}{4} L^4 \quad (4)$$

with  $a(x) = 6.75 - \frac{1.95}{x} + \frac{2.625}{x^2} - \frac{7.44}{x^3}$ . The feedbacks of quarks to gluons are also important and can be taken into account by modifying the deconfinement temperature  $T_0$  according to the corrections of the two-loop  $\beta$ -function of QCD [25], that is,

$$T_0 = T_\tau e^{-\frac{1/\alpha_s}{b(N_f, \mu_B)}}, \quad (5)$$

and

$$b(N_f, \mu_B) = \frac{33 - 2N_f}{6\pi} - \frac{16N_f}{\pi} \left( \frac{\mu_B}{2T_\tau} \right)^2, \quad (6)$$

with  $T_\tau = 1.77$  GeV,  $\alpha_s = 0.304$  and  $N_f = 3$ .

To accurately evaluate dilepton emission, the degrees of freedom of vector mesons should be taken into account since they very successfully capture the nonperturbative features of QCD in the hadronic phase [13]. Mainly, the

neutral mesons,  $\rho^0, \omega$  and  $\phi$ , are involved in calculating the dilepton production from charged pion annihilation in the vector dominance model [26, 27]. Among them,  $\rho^0$  is supposed to be the most sensitive channel to study the approximate  $SU(2)$  chiral symmetry breaking and restoration, because it is not chiral invariant and mostly decays to  $\pi^+ \pi^-$ . We will focus on the varying features of dilepton emission through  $\rho^0$  channel in the hadronic phase, and the lowest-lying vectors  $\rho^0, \rho^\pm$  and axial-vectors  $a_1^0, a_1^\pm$  are needed to keep the approximate  $SU(2)$  chiral symmetry of the model [18]. Then, the corrections from vector mesons to the Lagrangian are [18, 27]

$$\begin{aligned} \Delta \mathcal{L}_{\text{PQM}} = & -\frac{1}{4} (\rho_{\mu\nu}^b \rho_b^{\mu\nu} + a_{1\mu\nu}^b a_{1b}^{\mu\nu}) + \frac{m_\rho^2}{2} (\rho_\mu^b \rho_b^\mu + a_{1\mu}^b a_{1b}^\mu) \\ & + \bar{\psi} [g_{\text{vq}} T^b \gamma^\mu (\rho_{b\mu} + i\gamma^5 a_{1b\mu})] \psi + \mathcal{L}_{\text{sv}}, \end{aligned} \quad (7)$$

where the two terms in the first line are the kinetic and mass parts, respectively, and the first term in the second line indicates quark-(pseudo-)vector meson interactions. The scalar-vector interaction  $\mathcal{L}_{\text{sv}}$  can be introduced by taking the substitutions in the lightest flavor sector [18],  $\partial_\mu \sigma_1 \rightarrow (\mathcal{D}^\mu \sigma)_1 \equiv \partial_\mu \sigma_1 - g_{\text{sv}} a_{1\mu}^{b\dagger} \pi_b$  and  $\partial^\mu \pi^b \rightarrow (\mathcal{D}^\mu \pi)^b \equiv \partial_\mu \pi^b + g_{\text{sv}} (i\varepsilon^{bcd} \pi_c^\dagger \rho_{du}^\dagger + a_{1\mu}^b \sigma_1)$  with  $b, c, d = 1, 2, 3$  corresponding to the charges  $+, -, 0$ .

*Dilepton emission rate.* To transform the QCD signal to the dilepton emission rate, the QED theory for leptons is necessary and the Lagrangian is well-known,

$$\mathcal{L}_{\text{QED}} = -\frac{1}{4} F_{\mu\nu} F^{\mu\nu} + \sum_{l=e,\mu} \bar{l} [i\gamma^\mu (\partial_\mu + i e A_\mu) - m_l] l \quad (8)$$

with the EM strength tensor  $F_{\mu\nu} \equiv \partial_\mu A_\nu - \partial_\nu A_\mu$  and the light lepton field  $l = e, \mu$ . Eventually, dock the established chiral effective model to the QED theory with the help of  $\rho^0$ -photon interaction [13], the total Lagrangian can be summarized as

$$\mathcal{L} = \mathcal{L}_{\text{PQM}}^0 + \Delta \mathcal{L}_{\text{PQM}} + \mathcal{L}_{\text{QED}} - \frac{e}{g_{\text{sv}}} m_\rho^2 \rho_\mu^0 A^\mu. \quad (9)$$

In such a model, DERs receive contributions from two parts [12, 13]: perturbative quark-antiquark annihilations within QED and nonperturbative charged hadron annihilations through the  $\rho^0$  current, see the illustrations of the corresponding Feynman diagrams in Fig. 1. According to Ref. [12], the DER can be simply presented in terms of EM current correlation functions, which is

$$\frac{d^4 R}{d^4 q} = -\frac{\alpha^2}{6\pi^3} \frac{L_1}{M^2} \left( \frac{m_\rho^4}{g_{\text{sv}}^2} \frac{2 \text{Im}(D_{\rho^0}^R)^\mu_\mu}{e^{q^0/T} - 1} + N_c \sum_{f=u,d,s} W_{(f)\mu}^\mu \right) \quad (10)$$

by following the vector dominance model [26, 27] and accounting for the quark current [28]. Here, the simple function  $L_1(M^2) \equiv \sum_{l=e,\mu} \sqrt{1 - 4\tilde{m}_l^2} (1 + 2\tilde{m}_l^2)$  ( $\tilde{m} \equiv m/\sqrt{M^2}$ ) comes from the summations over spins and integrations over momenta of the final state dileptons [12],

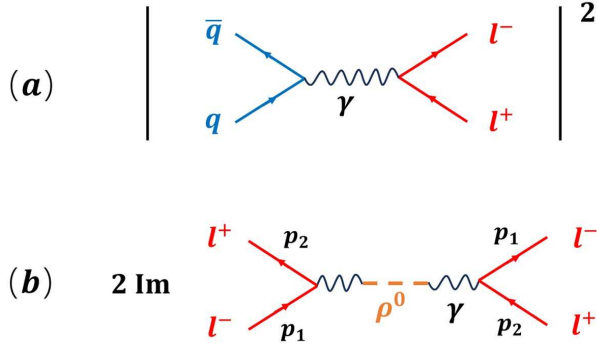


FIG. 1. The main dilepton production mechanisms in QCD matter: (a) direct quark-antiquark annihilations through QED, (b) indirect charged hadron annihilations in term of the imaginary part of the retarded propagator of  $\rho^0$  meson.

and  $D_{\rho^0}^R(q)$  is the retarded propagator of  $\rho^0$  meson. Compared to the simple mesonic model [27], there are extra contributions from quark loops in  $D_{\rho^0}^R(q)$  which could essentially account for the effect of chiral transition on  $\rho$  meson [29] and partially reflect the nonperturbative contributions from charged baryon annihilations [13], see the supplemental material for its expression and the detailed derivations.

The EM current correlation functions from quarks can be given explicitly as [12]

$$W_{(f)\mu}^\mu = -2 \left( \frac{q_f}{e} \right)^2 \int \frac{d^3 \mathbf{k}_1}{(2\pi)^3} \frac{n_f^+ (E_{\mathbf{k}_1}^f)}{2E_{\mathbf{k}_1}^f} \int \frac{d^3 \mathbf{k}_2}{(2\pi)^3} \frac{n_f^- (E_{\mathbf{k}_2}^f)}{2E_{\mathbf{k}_2}^f} (2\pi)^4 \delta^{(4)}(k_1 + k_2 - q) (k_1 \cdot k_2 + 2m_f^2), \quad (11)$$

where  $E_{\mathbf{k}}^f = \sqrt{\mathbf{k}^2 + m_f^2}$  are the quark or antiquark energies, and the corresponding distribution functions can be derived from the chiral effective model at mean field approximation as [17]

$$n_f^t(k) = \frac{L H_f^t + 2L (H_f^t)^2 + (H_f^t)^3}{1 + 3L H_f^t + 3L (H_f^t)^2 + (H_f^t)^3} \quad (12)$$

with the auxiliary function  $H_f^t(E_{\mathbf{k}}^f, \mu_B) \equiv e^{-\frac{1}{T}(E_{\mathbf{k}}^f - t \frac{\mu_B}{3})}$ . According to (12), the Polyakov loop  $L$  controls the effective fermion degrees of freedom in the QCD matter [30]: In the confined phase with  $L = 0$ ,  $n_f^t(p)$  would be reduced to the distribution functions for baryons and antibaryons; in the completely deconfined phase with  $L = 1$ ,  $n_f^t(p)$  are just the distribution functions for quarks and antiquarks. By following the integral tricks given in Ref. [27], we can get rid of the delta functions and angular variables in (11) to arrive at

$$W_{(f)\mu}^\mu = - \left( \frac{q_f}{e} \right)^2 \int_{k_-}^{k_+} \frac{k dk}{8\pi} n_f^+ (E_{\mathbf{k}}^f) n_f^- (q_0 - E_{\mathbf{k}}^f) \frac{M^2 + 2m_f^2}{|\mathbf{q}| E_{\mathbf{k}}^f} \quad (13)$$

with the upper/lower integral limits defined as  $k_\pm \equiv \frac{|\mathbf{q}|}{2} \left( 1 \pm \sqrt{1 + (1 - 4\tilde{q}_0^2 \tilde{m}_f^2)/|\mathbf{q}|^2} \right)$ .

The dilepton signals for QCD critical point. To carry out numerical calculations, we fix the parameters for PQM model as [17]

$$g_{sq} = 5.91, m_\phi = 435 \text{ MeV}, h_1 = -2.70, h_2 = 46.5, \kappa = 4810 \text{ MeV}, c_0 = (286 \text{ MeV})^3, c_8 = -(311 \text{ MeV})^3$$

which gives the  $\sigma_1$  mass  $m_{\sigma_1} = 500 \text{ MeV}$ , the pseudo-critical temperature  $T_{pc} = 159 \text{ MeV}$  at  $\mu_B = 0$  and the critical point  $(\mu_{Bc}, T_c) = (635, 93) \text{ MeV}$ . For the vector sector, we take the vacuum mass of  $\rho$  meson to be  $m_\rho = 770 \text{ MeV}$ , and fix  $g_{sv} = 6.07$  and  $g_{vq} = 1.55$  to reproduce the decay width  $\Gamma_\rho = 155 \text{ MeV}$  in the vacuum [27] and the location of DER peak ( $\sim m_\rho$ ) in high energy collision [31], respectively. To study the critical phenomena, we consider two realistic chemical freeze-out lines,  $T = 0.158 - 0.14\mu_B^2 - 0.04n\mu_B^4$  ( $n = 2, 3$ ) with the units GeV for both  $T$  and  $\mu_B$  [8]. Mainly, the numerical calculations can be divided into two steps: 1. Based on the mean field approximation, the quark masses, Polyakov loop, and pion mass are solved self-consistently from the coupled gap equations and two-body correlation function at given  $T$  and  $\mu_B$ . 2. Take the values of these physical quantities as input, the dilepton emission rate (10) can be evaluated numerically. Usually, researchers are more interested in the integrated dilepton emission rate [13], such as the one integrating over the momentum,

$$\mathcal{R} \equiv \frac{dR}{dM^2} = \int \frac{d^3 \mathbf{q}}{2q^0} \frac{d^4 R}{d^4 q} \Big|_{q_0 \rightarrow \sqrt{M^2 + \mathbf{q}^2}}. \quad (15)$$

Along the freezeout line with  $n = 2$  which is closer to the critical point, the integrated DERs  $\mathcal{R}$  are illustrated in Fig. 2 for several values of baryon chemical potential  $\mu_B$ . Since the temperature decreases with  $\mu_B$  along the freezeout line,  $\mathcal{R}$  also decreases with  $\mu_B$ . Compared to the baselines  $\mathcal{R}_0$ , the peaks of full DERs are slightly shifted to larger  $M$  – this is consistent with the lattice result that the screening mass of  $\rho$  meson would increase after chiral symmetry restoration [29]. Obviously, the deviations between the full DERs and baselines are more significant in the non-peak region than that in the peak region. The insertion shows that both the curvatures of the peak,  $\kappa_p \equiv \left| \frac{d^2 \mathcal{R}}{dM^2} \right|_{M_p}$ , decrease with  $\mu_B$ , consistent with the broadening phenomenon [13].

The dilepton emission around the peak was usually thought to be from the thermalized medium and far away from other nonthermal processes [12], such as the hard Drell-Yan process and the soft bremsstrahlung emission. In the following, we just focus on the peak of the DER,  $\mathcal{R}_p \equiv \mathcal{R}|_{M_p}$ , and show that the DER could well catch the chiral criticality. For that sake, we introduce dimensionless moments of the reduced light quark mass  $\tilde{m} \equiv$

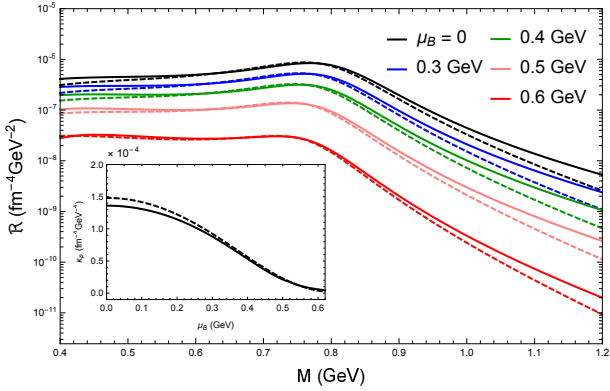


FIG. 2. Along the freezeout line with  $n = 2$ , the integrated dilepton emission rates  $\mathcal{R}$  as functions of the dilepton invariant mass  $M$  for several values of baryon chemical potential  $\mu_B$ . The solid lines are full DERs receiving contributions from both Fig. 1 (a) and (b), and the dashed ones are the baselines  $\mathcal{R}_0$  where only pions with fixed mass contribute [27]. The insertion are the curvatures  $\kappa_p$  of the DER peaks as functions of the baryon chemical potential  $\mu_B$  for the full calculation (solid line) and baseline (dashed line).

$m_1/m_1|_{\mu_B=0}$  and the reduced DER  $\tilde{\mathcal{R}}_p \equiv \mathcal{R}_p/\mathcal{R}_p|_{\mu_B=0}$  as

$$\tilde{m}_1^{(n)} \equiv \frac{\partial^n \tilde{m}_1}{\partial (\mu_B/T)^n}, \quad \tilde{\mathcal{R}}_p^{(n)} \equiv \frac{\partial^n \tilde{\mathcal{R}}_p}{\partial (\mu_B/T)^n} \quad (16)$$

with the temperature fixed at the freezeout point. The results are demonstrated altogether in Fig. 3 for  $n = 0, 1, 2, 3$  with respect to both  $\mu_B$  and the corresponding colliding energy  $\sqrt{S_{NN}}$  [8].

As one can see, up to a sign, the features of  $\tilde{\mathcal{R}}_p^{(n)}$  closely follow those of  $\tilde{m}_1^{(n)}$ ; especially for larger  $n$ , the locations of the extrema align with each other very well. In that sense, the DER indeed can well reflect the change of chiral symmetry and help to locate the critical point. Since the order parameter  $m_1$  is related to the first derivative of the pressure,  $S_m \sigma_m \equiv \tilde{m}_1^{(3)}/\tilde{m}_1'$  and  $S_R \sigma_R \equiv \tilde{\mathcal{R}}_p^{(3)}/\tilde{\mathcal{R}}_p'$  actually correspond to  $\kappa \sigma^2$  for baryon number fluctuations – that can be justified by their similar extremal structures except the pole regions of  $S_R \sigma_R$ . According to the Nambu–Jona-Lasinio model [8] and FRG-QCD [21], the peaks of  $\kappa \sigma^2$  is around 5, thus  $S_R \sigma_R$  is at least one order larger and serves as a more sensitive probe of critical point. Finally, when one shifts the freezeout line from  $n = 2$  to  $n = 3$ , the kink in  $\tilde{\mathcal{R}}_p^{(3)}$  around  $\mu_B \sim 0.3$  GeV becomes almost invisible, which indicates that the DER is also more sensitive to the relative location of the critical point.

Nevertheless, it is recently difficult to measure the higher moments of DER as the statistics is very poor in heavy ion collisions. Instead, we are able to better constrain the spectra of thermal DER for given freezeout points, such as those given in Fig. 2. The baselines are

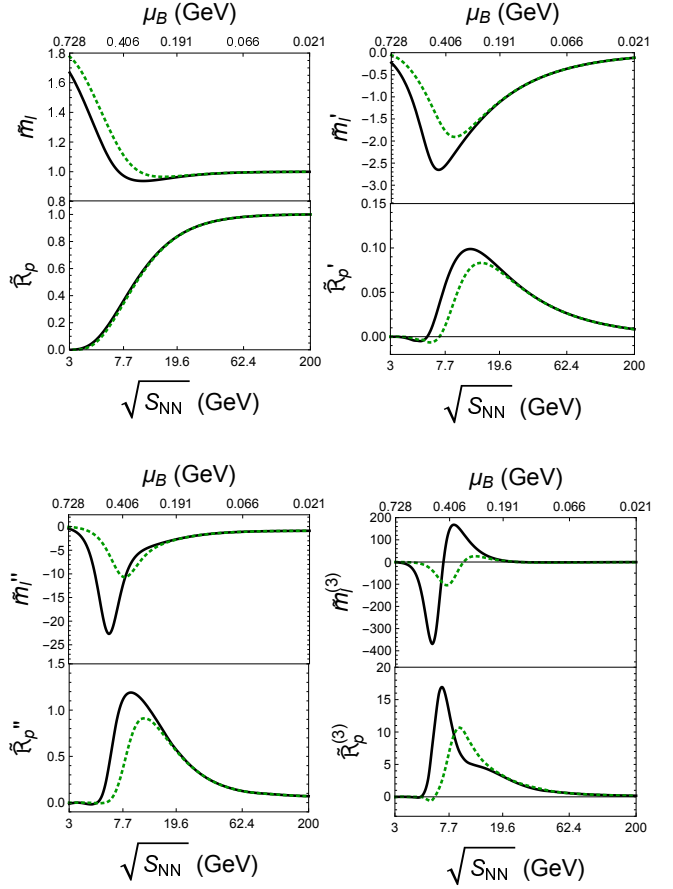


FIG. 3. A comparison between the moments of the reduced light quark mass,  $\tilde{m}_1^{(n)}$ , and those of reduced dilepton emission rate,  $\tilde{\mathcal{R}}_p^{(n)}$ , as functions of the baryon chemical potential  $\mu_B$  and colliding energy  $\sqrt{S_{NN}}$ . Here, the black solid and green dashed lines correspond to the freezeout lines  $n = 2$  and  $n = 3$ , respectively.

free of critical effects, so we can take the baseline subtracted DERs  $\Delta \mathcal{R}$  to explore criticality. Take two values of  $M$  away from the peak region for example, the results for the relative deviations,  $\Delta \mathcal{R}/\mathcal{R}_0$ , are illustrated in Fig. 4. As the effects are solely induced by quarks, the non-monotonic features can be regarded as alternative signals of QCD critical point. As we can see, the largest deviations show up around the point where the mass fluctuation  $\tilde{m}_1'$  is the strongest.

*Summary and discussions.* In this work, we propose dilepton emission as a novel and more sensitive probe of critical point. To demonstrate that, the well known Polyakov-quark-meson model is extended to include the vector sector, especially quark-vector and scalar-vector interactions, while maintaining the approximate  $SU(2)$  chiral symmetry. Such a model is capable of capturing two main mechanisms for dilepton production: At low temperature and baryon density, the QCD matter is in the hadronic phase where quarks are confined, so  $\pi^\pm$  an-

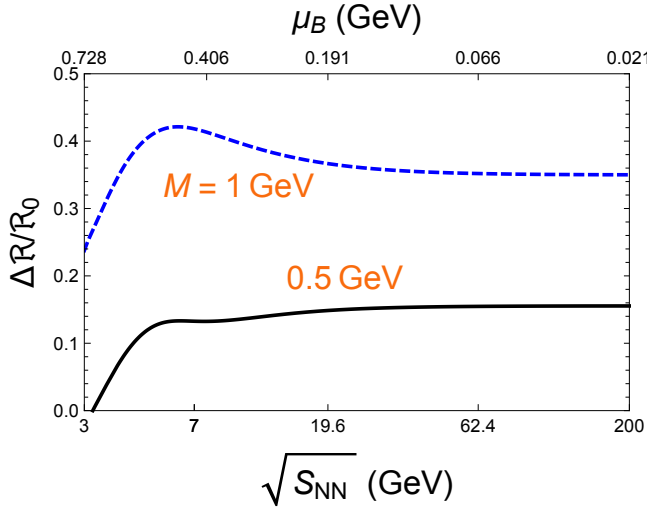


FIG. 4. The relative deviations of the full DERs from the baselines,  $\Delta\mathcal{R}/\mathcal{R}_0$ , as functions of the baryon chemical potential  $\mu_B$  and colliding energy  $\sqrt{s_{NN}}$  along the freezeout line  $n = 2$  for two center of masses,  $M = 0.5$  and  $1$  GeV.

nihilations dominate the contribution and the nonperturbative effect could be successfully accounted for through the vector dominance model. At high temperature and baryon density, the QCD matter is in the deconfined quark-gluon plasma phase due to asymptotic freedom, so quark-antiquark annihilations dominate the contribution and QED is accurate for perturbative calculations. In between, the chiral transition and (de-)confinement can be self-consistently explored within the model, and the predicted pseudocritical temperature and critical point are in good agreement with those from lattice QCD and functional QCD approaches. Thus, the extended PQM model is convincing to capture the main features of dilepton emission around the QCD critical region.

It is found that the dilepton emission rate decreases more and more drastically and the peak becomes flatter and flatter with the baryon chemical potential increasing along the chemical freezeout line. The peak region mainly receives contribution from the thermalized QCD medium hence is ideal for the study of critical effect. All the moments of the DER peak show similar extremal features as those of light quark mass, thus the DER can well reflect the change of chiral symmetry and help to locate the critical point. In contrary to the quark mass, the moments of DER in principle can be directly measured in heavy ion collisions, that is,  $\sim \langle \delta\mathcal{R}(\delta\hat{N}_B)^n \rangle$ . And compared to the usual baryon number fluctuations, the DER fluctuations are more drastic in the critical region and more sensitive to the relative location of critical point. However, recent statistics is not large enough to perform event-by-event measurement in heavy ion collisions, so we look forward to the CBM experiment with higher illumination in the future. In the short term, we propose the

baseline subtracted DER as an alternative signal: For a given dilepton center of mass, the largest deviation shows up around the point where the mass fluctuation  $\tilde{m}'_1$  is the strongest..

*Acknowledgement* G.C. thanks C. Yang from Shandong University for helpful discussions in many occasions. The work is funded by the Forefront Leading Project of Theoretical Physics from the National Natural Science Foundation of China with Grant No. 12447102. G.C. is also supported by the Natural Science Foundation of Guangdong Province with Grant No. 2024A1515011225. X.F.L. is also supported by the National Natural Science Foundation of China with Grant Nos. 12122505, 11890711, and the National Key Research and Development Program of China with contract Nos. 2022YFA1604900, 2020YFE0202002, 2018YFE0205201. W.J.F. is also supported by the National Natural Science Foundation of China with Grant No. 12175030.

\* caogaoqing@sysu.edu.cn

† xfluo@ccnu.edu.cn

‡ wjfu@dlut.edu.cn

- [1] M. S. Abdallah *et al.* (STAR), Measurements of Proton High Order Cumulants in  $\sqrt{s_{NN}} = 3$  GeV Au+Au Collisions and Implications for the QCD Critical Point, *Phys. Rev. Lett.* **128**, 202303 (2022), arXiv:2112.00240 [nucl-ex].
- [2] M. Abdallah *et al.* (STAR), Higher-order cumulants and correlation functions of proton multiplicity distributions in  $s_{NN}=3$  GeV Au+Au collisions at the RHIC STAR experiment, *Phys. Rev. C* **107**, 024908 (2023), arXiv:2209.11940 [nucl-ex].
- [3] B. E. Aboona *et al.* (STAR), Precision Measurement of Net-Proton-Number Fluctuations in Au+Au Collisions at RHIC, *Phys. Rev. Lett.* **135**, 142301 (2025), arXiv:2504.00817 [nucl-ex].
- [4] M. A. Stephanov, On the sign of kurtosis near the QCD critical point, *Phys. Rev. Lett.* **107**, 052301 (2011), arXiv:1104.1627 [hep-ph].
- [5] W.-j. Fu, X. Luo, J. M. Pawłowski, F. Rennecke, R. Wen, and S. Yin, Hyper-order baryon number fluctuations at finite temperature and density, *Phys. Rev. D* **104**, 094047 (2021), arXiv:2101.06035 [hep-ph].
- [6] W.-j. Fu, X. Luo, J. M. Pawłowski, F. Rennecke, and S. Yin, Ripples of the QCD critical point, *Phys. Rev. D* **111**, L031502 (2025), arXiv:2308.15508 [hep-ph].
- [7] Y. Lu, F. Gao, Y.-x. Liu, and J. M. Pawłowski, Finite density signatures of confining and chiral dynamics in QCD thermodynamics and fluctuations of conserved charges, (2025), arXiv:2504.05099 [hep-ph].
- [8] X. Luo and N. Xu, Search for the QCD Critical Point with Fluctuations of Conserved Quantities in Relativistic Heavy-Ion Collisions at RHIC : An Overview, *Nucl. Sci. Tech.* **28**, 112 (2017), arXiv:1701.02105 [nucl-ex].

[9] X. Luo, Q. Wang, N. Xu, and P. Zhuang, eds., *Properties of QCD Matter at High Baryon Density* (Springer, 2022).

[10] N. Dupuis, L. Canet, A. Eichhorn, W. Metzner, J. M. Pawłowski, M. Tissier, and N. Wschebor, The nonperturbative functional renormalization group and its applications, *Phys. Rept.* **910**, 1 (2021), arXiv:2006.04853 [cond-mat.stat-mech].

[11] W.-j. Fu, QCD at finite temperature and density within the fRG approach: an overview, *Commun. Theor. Phys.* **74**, 097304 (2022), arXiv:2205.00468 [hep-ph].

[12] L. D. McLerran and T. Toimela, Photon and Dilepton Emission from the Quark - Gluon Plasma: Some General Considerations, *Phys. Rev. D* **31**, 545 (1985).

[13] R. Rapp and J. Wambach, Chiral symmetry restoration and dileptons in relativistic heavy ion collisions, *Adv. Nucl. Phys.* **25**, 1 (2000), arXiv:hep-ph/9909229.

[14] M. Stephanov, Non-Gaussian fluctuations near the QCD critical point, *Phys. Rev. Lett.* **102**, 032301 (2009), arXiv:0809.3450 [hep-ph].

[15] L. D. McLerran, A Chiral Symmetry Order Parameter, the Lattice and Nucleosynthesis, *Phys. Rev. D* **36**, 3291 (1987).

[16] B.-J. Schaefer, M. Wagner, and J. Wambach, Thermodynamics of (2+1)-flavor QCD: Confronting Models with Lattice Studies, *Phys. Rev. D* **81**, 074013 (2010), arXiv:0910.5628 [hep-ph].

[17] G. Cao, Moat regimes within a (2+1)-flavor Polyakov-quark-meson model, *Phys. Rev. D* **112**, 034013 (2025), arXiv:2504.18874 [hep-ph].

[18] R. D. Pisarski, Where does the rho go? Chirally symmetric vector mesons in the quark - gluon plasma, *Phys. Rev. D* **52**, R3773 (1995), arXiv:hep-ph/9503328.

[19] R. Bellwied, S. Borsanyi, Z. Fodor, J. Guenther, S. D. Katz, C. Ratti, and K. K. Szabo, The QCD phase diagram from analytic continuation, *Phys. Lett. B* **751**, 559 (2015), arXiv:1507.07510 [hep-lat].

[20] A. Bazavov *et al.* (HotQCD), Chiral crossover in QCD at zero and non-zero chemical potentials, *Phys. Lett. B* **795**, 15 (2019), arXiv:1812.08235 [hep-lat].

[21] W.-j. Fu, J. M. Pawłowski, and F. Rennecke, QCD phase structure at finite temperature and density, *Phys. Rev. D* **101**, 054032 (2020), arXiv:1909.02991 [hep-ph].

[22] F. Gao and J. M. Pawłowski, Chiral phase structure and critical end point in QCD, *Phys. Lett. B* **820**, 136584 (2021), arXiv:2010.13705 [hep-ph].

[23] P. J. Gunkel and C. S. Fischer, Locating the critical endpoint of QCD: Mesonic backcoupling effects, *Phys. Rev. D* **104**, 054022 (2021), arXiv:2106.08356 [hep-ph].

[24] C. Ratti, M. A. Thaler, and W. Weise, Phases of QCD: Lattice thermodynamics and a field theoretical model, *Phys. Rev. D* **73**, 014019 (2006), arXiv:hep-ph/0506234 [hep-ph].

[25] T. K. Herbst, J. M. Pawłowski, and B.-J. Schaefer, The phase structure of the Polyakovquarkmeson model beyond mean field, *Phys. Lett. B* **696**, 58 (2011), arXiv:1008.0081 [hep-ph].

[26] G. J. Gounaris and J. J. Sakurai, Finite width corrections to the vector meson dominance prediction for  $\rho \rightarrow e^+e^-$ , *Phys. Rev. Lett.* **21**, 244 (1968).

[27] C. Gale and J. I. Kapusta, Vector dominance model at finite temperature, *Nucl. Phys. B* **357**, 65 (1991).

[28] K. Kajantie, J. I. Kapusta, L. D. McLerran, and A. Mekjian, Dilepton Emission and the QCD Phase Transition in Ultrarelativistic Nuclear Collisions, *Phys. Rev. D* **34**, 2746 (1986).

[29] A. Bazavov *et al.*, Meson screening masses in (2+1)-flavor QCD, *Phys. Rev. D* **100**, 094510 (2019), arXiv:1908.09552 [hep-lat].

[30] K. Fukushima, Chiral effective model with the Polyakov loop, *Phys. Lett. B* **591**, 277 (2004), arXiv:hep-ph/0310121 [hep-ph].

[31] Y. Han (STAR), Thermal dielectron measurements in Au+Au collisions at  $\sqrt{s_{NN}} = 7.7$ , 14.6, and 19.6 GeV with the STAR experiment, *EPJ Web Conf.* **296**, 07004 (2024).

# Supplemental materials for “Dilepton emission as a novel probe of QCD critical point”

Gaoqing Cao,<sup>1,\*</sup> Xiaofeng Luo,<sup>2,†</sup> and Wei-jie Fu<sup>3,‡</sup>

<sup>1</sup>*School of Physics and Astronomy, Sun Yat-sen University, Zhuhai 519088, China*

<sup>2</sup>*Key Laboratory of Quark & Lepton Physics (MOE) and Institute of Particle Physics, Central China Normal University, Wuhan 430079, China*

<sup>3</sup>*School of Physics, Dalian University of Technology, Dalian, 116024, China*

(Dated: January 1, 2026)

## THE DRESSED PROPAGATOR OF $\rho^0$ MESON

In the extended Polyakov-quark-meson model, the propagator of  $\rho^0$  meson receives corrections from both charged pion and quark loops as demonstrated in Fig. 5. At one-loop approximation, the Feynman diagrams can be translated

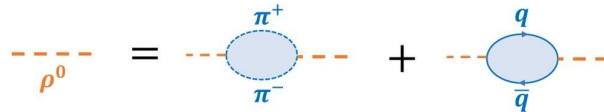


FIG. 5. The self-consistent Feynman diagrams for the dressed propagator of  $\rho^0$  meson (thick dashed line) in terms of its bare propagator (thin dashed line), charged pion loop (dotted loop) and quark loops (arrowed solid loop).

into mathematical expression for the inverse dressed propagator of  $\rho^0$  meson,  $(\mathcal{D}_{\rho^0}^{-1})^{\mu\nu}(q)$ , as

$$(\mathcal{D}_{\rho^0}^{-1})^{\mu\nu}(q) = (q^2 - m_\rho^2)g^{\mu\nu} - q^\mu q^\nu + \Pi_{\rho^0}^{\mu\nu}(q) = [F(q) - q^2] \mathcal{P}_L^{\mu\nu} + [G(q) - q^2] \mathcal{P}_t^{\mu\nu} - m_\rho^2 g^{\mu\nu}. \quad (17)$$

Here, the self-energy  $\Pi_{\rho^0}^{\mu\nu}(q)$  are composed of the contributions from charged pion loops  $\Pi_{\rho^0\pi}^{\mu\nu}(q)$  and quark loops  $\Pi_{\rho^0q}^{\mu\nu}(q)$ , that is,  $\Pi_{\rho^0}^{\mu\nu}(q) = \Pi_{\rho^0\pi}^{\mu\nu}(q) + \Pi_{\rho^0q}^{\mu\nu}(q)$ . Due to the violation of Lorentz invariance but intact of spatial rotational invariance at finite temperature and baryon chemical potential, the propagator is further separated into transverse and longitudinal polarized parts in the second step with the polarization tensors [27]

$$\mathcal{P}_t^{00} = \mathcal{P}_t^{0i} = \mathcal{P}_t^{i0} = 0, \quad \mathcal{P}_t^{ij} = -(g^{ij} + q^i q^j / \mathbf{q}^2), \quad \mathcal{P}_L^{\mu\nu} = q^\mu q^\nu / q^2 - g^{\mu\nu} - \mathcal{P}_t^{\mu\nu} \quad (i, j = 1, 2, 3). \quad (18)$$

The auxiliary functions are given by  $F(q) = (q^2 / \mathbf{q}^2) \Pi_{\rho^0}^{00}$  and  $G(q) = \mathcal{P}_{Tij} \Pi_{\rho^0}^{ij} / 2$ , which, similar to the self-energy, also receive contributions from both charged pion loops and quark loops, so we can separate them as  $F(q) = F_\pi(q) + F_q(q)$  and  $G(q) = G_\pi(q) + G_q(q)$ . Then, the dressed  $\rho^0$  propagator can be derived as [27]

$$\mathcal{D}_{\rho^0}^{\mu\nu}(q) = -\frac{\mathcal{P}_L^{\mu\nu}}{q^2 - m_\rho^2 - F(q)} - \frac{\mathcal{P}_t^{\mu\nu}}{q^2 - m_\rho^2 - G(q)} - \frac{q^\mu q^\nu}{m_\rho^2 q^2}, \quad (19)$$

and the retarded one is given by  $(\mathcal{D}_{\rho^0}^R)^{\mu\nu}(q) \equiv \mathcal{D}_{\rho^0}^{\mu\nu}(q)|_{q_0 \rightarrow E+i0^+}$  with  $E$  a positive energy. Eventually, the imaginary part of the retarded propagator, which is directly related to dilepton production, can be evaluated after taking trace over the Lorentz indices as

$$\text{Im} (\mathcal{D}_{\rho^0}^R)^\mu_\mu(q) = \frac{\text{Im} F(q)}{[q^2 - m_\rho^2 - \text{Re} F(q)]^2 + [\text{Im} F(q)]^2} + \frac{2 \text{Im} G(q)}{[q^2 - m_\rho^2 - \text{Re} G(q)]^2 + [\text{Im} G(q)]^2}. \quad (20)$$

The auxiliary functions from pion loops had been calculated in Ref. [27], where they were decomposed into vacuum

and thermal parts,  $F_\pi(q) = F_\pi^v(q) + F_\pi^t(q)$  and  $G_\pi(q) = G_\pi^v(q) + G_\pi^t(q)$ . The involved functions are

$$F_\pi^v = G_\pi^v = \frac{g_{sv}^2 M^2}{48\pi^2} \left[ (1-4\tilde{m}_\pi^2)^{\frac{3}{2}} \left( \ln \left| \frac{\sqrt{1-4\tilde{m}_\pi^2}+1}{\sqrt{1-4\tilde{m}_\pi^2}-1} \right| - i\pi \theta(1-4\tilde{m}_\pi^2) \right) + 8\tilde{m}_\pi^2 - \frac{8m_\pi^2}{m_\rho^2} - \left(1 - \frac{4m_\pi^2}{m_\rho^2}\right)^{\frac{3}{2}} \ln \left| \frac{\sqrt{1-\frac{4m_\pi^2}{m_\rho^2}}+1}{\sqrt{1-\frac{4m_\pi^2}{m_\rho^2}}-1} \right| \right], \quad (21)$$

$$F_\pi^t = \frac{g_{sv}^2 M^2}{4\pi^2 |\mathbf{q}|^2} \int_0^\infty \frac{k^2 dk}{E_\pi} \frac{1}{e^{E_\pi/T} - 1} \left[ \frac{4E_\pi^2 + E^2}{2k|\mathbf{q}|} (\ln |\alpha_\pi| - i\pi\Delta_\pi) + \frac{2E_\pi E}{k|\mathbf{q}|} (\ln |\beta_\pi| + i\pi\Delta_\pi) - 4 \right], \quad (22)$$

$$G_\pi^t = \frac{g_{sv}^2}{4\pi^2} \int_0^\infty \frac{k^2 dk}{E_\pi} \frac{1}{e^{E_\pi/T} - 1} \left[ \frac{4(|\mathbf{q}|^2 k^2 - E_\pi^2 E^2) - M^4}{4k|\mathbf{q}|^3} (\ln |\alpha_\pi| - i\pi\Delta_\pi) - \frac{E_\pi E M^2}{k|\mathbf{q}|^3} (\ln |\beta_\pi| + i\pi\Delta_\pi) + \frac{2M^2}{|\mathbf{q}|^2} + 4 \right] \quad (23)$$

with  $E_\pi = \sqrt{k^2 + m_\pi^2}$ ,  $E = \sqrt{|\mathbf{q}|^2 + M^2}$  and the auxiliary functions

$$\alpha_\pi \equiv \frac{(M^2 + 2k|\mathbf{q}|)^2 - 4E_\pi^2 E^2}{(M^2 - 2k|\mathbf{q}|)^2 - 4E_\pi^2 E^2}, \quad \beta_\pi \equiv \frac{M^4 - 4(k|\mathbf{q}| + E_\pi E)^2}{M^4 - 4(k|\mathbf{q}| - E_\pi E)^2}, \quad (24)$$

$$\Delta_\pi = \text{Boole}(|E\sqrt{1-4\tilde{m}_\pi^2} - |\mathbf{q}|| \leq 2k \leq E\sqrt{1-4\tilde{m}_\pi^2} + |\mathbf{q}|). \quad (25)$$

In the following, we will devote ourselves to deriving the self-energy  $\Pi_{\rho^0 q}^{\mu\nu}(q)$  and the corresponding auxiliary functions,  $F_q(q)$  and  $G_q(q)$ , from quark loops.

### The self-energy from quark loops

The self-energy from quark loops can be evaluated according to the second Feynman diagram on the right-hand side of Fig. 5 as

$$\Pi_{\rho^0 q}^{\mu\nu}(q) = -\frac{g_{vq}^2}{4V_4} \sum_{f=u,d}^{c=r,g,b} \text{tr} [G_{f,c}(k+q)\gamma^\mu G_{f,c}(k)\gamma^\nu], \quad (26)$$

where the traces  $\text{tr}$  are over Dirac matrices and energy momentum space, and the quark propagators are given at mean field approximation as [17]

$$G_{f,c}(k) = \frac{i}{-\not{k} - i\gamma^4 (iq_c T + \frac{\mu_B}{3}) - m_f} \quad (27)$$

with flavor indices  $f = u, d, s$ , color indices  $c = 1, 2, 3$ , and  $q_c$  the color charge. To account for effects of finite temperature and baryon chemical potential, it is simpler to work in Euclidean space. Then, after completing traces over Dirac matrices by utilizing the theorem  $\text{tr} \gamma^\mu \gamma^\rho \gamma^\nu \gamma^\sigma = 4(g^{\mu\rho}g^{\nu\sigma} - g^{\mu\nu}g^{\rho\sigma} + g^{\mu\sigma}g^{\nu\rho})$  and Matsubara frequency summation, the self-energy can be separated into a divergent vacuum term  $\Pi_{\rho^0 q(v)}^{\mu\nu}(q)$  and a convergent thermal term  $\Pi_{\rho^0 q(t)}^{\mu\nu}(q)$  with the forms

$$\Pi_{\rho^0 q(v)}^{\mu\nu}(q) = -\frac{3g_{vq}^2}{4} \sum_{f=u,d} \int \frac{d^4 k}{(2\pi)^4} \text{tr} \left[ \frac{i}{-\not{k} - \not{q} - m_f} \gamma^\mu \frac{i}{-\not{k} - m_f} \gamma^\nu \right], \quad (28)$$

$$\begin{aligned} \Pi_{\rho^0 q(t)}^{\mu\nu}(q) &= \frac{g_{vq}^2}{2} \sum_{f=u,d}^{c=r,g,b} \int \frac{d^3 \mathbf{k}}{(2\pi)^3} \sum_{u,t=\pm} \frac{1}{E_{\mathbf{k}+u\frac{\mathbf{q}}{2}}^f \left[ (E_{\mathbf{k}+u\frac{\mathbf{q}}{2}}^f + u t i q_4)^2 - (\mathbf{k} - u \frac{\mathbf{q}}{2})^2 - m_f^2 \right]} \frac{1}{1 + e^{\left[ E_{\mathbf{k}+u\frac{\mathbf{q}}{2}}^f - t(iq_c T + \frac{\mu_B}{3}) \right]/T}} \\ &\quad \left\{ \left[ -E_{\mathbf{k}+u\frac{\mathbf{q}}{2}}^f (E_{\mathbf{k}+u\frac{\mathbf{q}}{2}}^f + u t i q_4) + \mathbf{k}^2 - \frac{\mathbf{q}^2}{4} + m_f^2 \right] g^{\mu\nu} + \left[ i t E_{\mathbf{k}+u\frac{\mathbf{q}}{2}}^f g^{4\mu} + \left( \mathbf{k} + u \frac{\mathbf{q}}{2} \right)^\mu \right] \left[ (i t E_{\mathbf{k}+u\frac{\mathbf{q}}{2}}^f - u q_4) g^{4\nu} \right. \right. \\ &\quad \left. \left. + \left( \mathbf{k} - u \frac{\mathbf{q}}{2} \right)^\nu \right] + \left[ i t E_{\mathbf{k}+u\frac{\mathbf{q}}{2}}^f g^{4\nu} + \left( \mathbf{k} + u \frac{\mathbf{q}}{2} \right)^\nu \right] \left[ (i t E_{\mathbf{k}+u\frac{\mathbf{q}}{2}}^f - u q_4) g^{4\mu} + \left( \mathbf{k} - u \frac{\mathbf{q}}{2} \right)^\mu \right] \right\}. \end{aligned} \quad (29)$$

Here, the quark energies are defined as  $E_{\mathbf{k}}^f \equiv \sqrt{\mathbf{k}^2 + m_f^2}$ .

One could immediately recognize that the vacuum term is exactly the same as that for photon polarization except the coupling constant. So by following the standard dimensional regularization in textbooks and applying the renormalization condition  $\text{Im} \Pi_{\rho^0 q(v)}^{\mu\nu}(q) = 0$  and  $\text{Re} \Pi_{\rho^0 q(v)}^{\mu\nu} \Big|_{m_f \rightarrow m_{f0}}^{q^2 \rightarrow m_\rho^2} = 0$ , which means  $\rho^0$  cannot decay into quark-antiquark

pair for any  $q^2$  and the self-energy vanishes at  $q^2 = m_\rho^2$  in vacuum, we have

$$\begin{aligned}
\Pi_{\rho^0 q(v)}^{\mu\nu}(q) &= -(q^2 g^{\mu\nu} - q^\mu q^\nu) \frac{3g_{vq}^2}{8\pi^2} \sum_{f=u,d} \int_0^1 dx \ x(1-x) \text{Re} \ln \left( \frac{m_f^2 - x(1-x)q^2}{m_{f0}^2 - x(1-x)m_\rho^2} \right) \\
&= -(q^2 g^{\mu\nu} - q^\mu q^\nu) \frac{g_{vq}^2}{16\pi^2} \sum_{f=u,d} \text{Re} \left[ \ln \frac{m_f^2 m_\rho^2}{m_{f0}^2 q^2} - 4 \left( \frac{m_f^2}{q^2} - \frac{m_{f0}^2}{m_\rho^2} \right) + \sqrt{1 - \frac{4m_f^2}{q^2}} \left( 1 + \frac{2m_f^2}{q^2} \right) \ln \frac{\sqrt{1 - \frac{4m_f^2}{q^2}} + 1}{\sqrt{1 - \frac{4m_f^2}{q^2}} - 1} \right. \\
&\quad \left. - \sqrt{1 - \frac{4m_{f0}^2}{m_\rho^2}} \left( 1 + \frac{2m_{f0}^2}{m_\rho^2} \right) \ln \frac{\sqrt{1 - \frac{4m_{f0}^2}{m_\rho^2}} + 1}{\sqrt{1 - \frac{4m_{f0}^2}{m_\rho^2}} - 1} \right]. \tag{30}
\end{aligned}$$

In Minkowski space, the contributions to the self-energies of longitudinal and transverse polarized  $\rho^0$  mesons are both

$$\begin{aligned}
F_q^v &= G_q^v = \frac{g_{vq}^2 M^2}{16\pi^2} \sum_{f=u,d} \text{Re} \left[ \ln \frac{\tilde{m}_f^2 m_\rho^2}{m_{f0}^2} - 4(\tilde{m}_f^2 - \frac{m_{f0}^2}{m_\rho^2}) + \sqrt{1 - 4\tilde{m}_f^2} (1 + 2\tilde{m}_f^2) \ln \frac{\sqrt{1 - 4\tilde{m}_f^2} + 1}{\sqrt{1 - 4\tilde{m}_f^2} - 1} \right. \\
&\quad \left. - \sqrt{1 - \frac{4m_{f0}^2}{m_\rho^2}} \left( 1 + \frac{2m_{f0}^2}{m_\rho^2} \right) \ln \frac{\sqrt{1 - \frac{4m_{f0}^2}{m_\rho^2}} + 1}{\sqrt{1 - \frac{4m_{f0}^2}{m_\rho^2}} - 1} \right]. \tag{31}
\end{aligned}$$

### The thermal part of the self-energy from quark loops

Now, we focus on the thermal term which can be reduced to a more compact form as the following

$$\begin{aligned}
\Pi_{\rho^0 q(t)}^{\mu\nu}(q) &= \frac{3g_{vq}^2}{2} \sum_{f=u,d} \int \frac{d^3 \mathbf{k}}{(2\pi)^3} \sum_{u,t=\pm} \frac{n_f^t(\mathbf{k} + \frac{\mathbf{q}}{2})}{E_{\mathbf{k}+\frac{\mathbf{q}}{2}}^f [2u t E_{\mathbf{k}+\frac{\mathbf{q}}{2}}^f(iq_4) + 2\mathbf{q} \cdot \mathbf{k} + (iq_4)^2]} \left\{ \left[ -u t E_{\mathbf{k}+\frac{\mathbf{q}}{2}}^f(iq_4) - \mathbf{q} \cdot \mathbf{k} - \frac{\mathbf{q}^2}{2} \right] g^{\mu\nu} \right. \\
&\quad \left. + 2 \left[ (i u t E_{\mathbf{k}+\frac{\mathbf{q}}{2}}^f - \frac{q_4}{2}) g^{4\mu} + \mathbf{k}^\mu \right] \left[ (i u t E_{\mathbf{k}+\frac{\mathbf{q}}{2}}^f - \frac{q_4}{2}) g^{4\nu} + \mathbf{k}^\nu \right] - \frac{q^\mu q^\nu}{2} \right\} \\
&= -\frac{3g_{vq}^2}{2} \left[ g^{\mu\nu} + \left( 1 - \frac{\mathbf{q}^2}{q_4^2} \right) g^{4\mu} g^{4\nu} + g^{4\mu} \frac{\mathbf{q}^\nu}{q_4} + g^{4\nu} \frac{\mathbf{q}^\mu}{q_4} \right] \sum_{f=u,d} \int \frac{d^3 \mathbf{k}}{(2\pi)^3} \sum_{t=\pm} \frac{n_f^t(\mathbf{k} + \frac{\mathbf{q}}{2})}{E_{\mathbf{k}+\frac{\mathbf{q}}{2}}^f} \\
&\quad + \frac{3g_{vq}^2}{4} \sum_{f=u,d} \int \frac{d^3 \mathbf{k}}{(2\pi)^3} \sum_{u,t=\pm} \frac{q^2 g^{\mu\nu} - q^\mu q^\nu + 4 \left( \frac{\mathbf{q} \cdot \mathbf{k}}{q_4} g^{4\mu} - \mathbf{k}^\mu \right) \left( \frac{\mathbf{q} \cdot \mathbf{k}}{q_4} g^{4\nu} - \mathbf{k}^\nu \right)}{E_{\mathbf{k}+\frac{\mathbf{q}}{2}}^f [2u t E_{\mathbf{k}+\frac{\mathbf{q}}{2}}^f(iq_4) + 2\mathbf{q} \cdot \mathbf{k} + (iq_4)^2]} n_f^t \left( \mathbf{k} + \frac{\mathbf{q}}{2} \right) \\
&= -\frac{3g_{vq}^2}{2} \left[ g^{\mu\nu} + \left( 1 - \frac{\mathbf{q}^2}{q_4^2} \right) g^{4\mu} g^{4\nu} + g^{4\mu} \frac{\mathbf{q}^\nu}{q_4} + g^{4\nu} \frac{\mathbf{q}^\mu}{q_4} \right] \sum_{f=u,d} \int \frac{d^3 \mathbf{k}}{(2\pi)^3} \sum_{t=\pm} \frac{n_f^t(\mathbf{k})}{E_{\mathbf{k}}^f} \\
&\quad + \frac{3g_{vq}^2}{4} \sum_{f=u,d} \int \frac{d^3 \mathbf{k}}{(2\pi)^3} \sum_{u,t=\pm} \frac{q^2 g^{\mu\nu} - q^\mu q^\nu + \left( \frac{2\mathbf{q} \cdot \mathbf{k} - \mathbf{q}^2}{q_4} g^{4\mu} - 2\mathbf{k}^\mu + \mathbf{q}^\mu \right) \left( \frac{2\mathbf{q} \cdot \mathbf{k} - \mathbf{q}^2}{q_4} g^{4\nu} - 2\mathbf{k}^\nu + \mathbf{q}^\nu \right)}{[2u t E_{\mathbf{k}}^f(iq_4) + 2\mathbf{q} \cdot \mathbf{k} + q^2]} \frac{n_f^t(\mathbf{k})}{E_{\mathbf{k}}^f}. \tag{32}
\end{aligned}$$

During the derivations, the tricks utilized are as follows: In the first step, the color degree of freedom is summed over to give rise to the particle distribution functions  $n_f^t(\mathbf{k}) \equiv \left[ L H_f^t + 2L(H_f^t)^2 + (H_f^t)^3 \right] \left[ 1 + 3L H_f^t + 3L(H_f^t)^2 + (H_f^t)^3 \right]^{-1}$  with  $H_f^t(E_{\mathbf{k}}^f, \mu_B) \equiv e^{-\frac{1}{T}(E_{\mathbf{k}}^f - t\frac{\mu_B}{3})}$ , and the momentum has been changed from  $\mathbf{k}$  to  $u \mathbf{k}$  in the integrand. In the second step, we try to simplify the formula by getting rid of the energy term  $E_{\mathbf{k}+\frac{\mathbf{q}}{2}}^f$  in the numerator. In the last step, we shift  $\mathbf{k} + \frac{\mathbf{q}}{2}$  to  $\mathbf{k}$  in the integrands in order to use odd-evenness to reduce the formula later.

In the following, we will try to separate the longitudinal part from the transverse part and then complete the integrations over solid angles to facilitate numerical calculations. Firstly, the most central component of the longitudinal

part is the temporal diagonal term,  $\Pi_{\rho^0 q(t)}^{44}(q)$ , which can be further reduced from (32) as

$$\begin{aligned} \Pi_{\rho^0 q(t)}^{44}(q) &= \frac{3g_{vq}^2}{2} \frac{\mathbf{q}^2}{q_4^2} \sum_{f=u,d} \int \frac{d^3 \mathbf{k}}{(2\pi)^3} \sum_{t=\pm} \frac{n_f^t(\mathbf{k})}{E_{\mathbf{k}}^f} + \frac{3g_{vq}^2}{4} \sum_{f=u,d} \int \frac{d^3 \mathbf{k}}{(2\pi)^3} \sum_{u,t=\pm} \frac{\mathbf{q}^2 + \left(\frac{2\mathbf{q} \cdot \mathbf{k} - \mathbf{q}^2}{q_4}\right)^2}{[2u t E_{\mathbf{k}}^f(iq_4) + 2\mathbf{q} \cdot \mathbf{k} + q^2]} \frac{n_f^t(\mathbf{k})}{E_{\mathbf{k}}^f} \\ &= \frac{3g_{vq}^2}{2} \sum_{f=u,d} \int \frac{d^3 \mathbf{k}}{(2\pi)^3} \sum_{t=\pm} \frac{n_f^t(\mathbf{k})}{E_{\mathbf{k}}^f} + \frac{3g_{vq}^2}{4} \sum_{f=u,d} \int \frac{d^3 \mathbf{k}}{(2\pi)^3} \sum_{u,t=\pm} \frac{\mathbf{q}^2 + \left(q_4 - 2i u t E_{\mathbf{k}}^f\right)^2}{[2u t E_{\mathbf{k}}^f(iq_4) + 2\mathbf{q} \cdot \mathbf{k} + q^2]} \frac{n_f^t(\mathbf{k})}{E_{\mathbf{k}}^f} \\ &= \frac{3g_{vq}^2}{2} \sum_{f=u,d} \int \frac{d^3 \mathbf{k}}{(2\pi)^3} \sum_{t=\pm} \frac{n_f^t(\mathbf{k})}{E_{\mathbf{k}}^f} - \frac{3g_{vq}^2}{4} \sum_{f=u,d} \int \frac{d^3 \mathbf{k}}{(2\pi)^3} \sum_{u,t=\pm} \frac{4\left(E_{\mathbf{k}}^f\right)^2 + q^2 + 4u t E_{\mathbf{k}}^f(iq_4)}{[2u t E_{\mathbf{k}}^f(iq_4) + 2\mathbf{q} \cdot \mathbf{k} + q^2]} \frac{n_f^t(\mathbf{k})}{E_{\mathbf{k}}^f} \\ &= -\frac{3g_{vq}^2}{8} \sum_{f=u,d} \int \frac{k dk}{(2\pi)^2 |\mathbf{q}|} \sum_{t=\pm} \left[ -8|\mathbf{q}|k + \left(4\left(E_{\mathbf{k}}^f\right)^2 + q^2\right) \ln \alpha_f^E + 4E_{\mathbf{k}}^f(iq_4) \ln \beta_f^E \right] \frac{n_f^t(\mathbf{k})}{E_{\mathbf{k}}^f}, \end{aligned} \quad (33)$$

$$\alpha_f^E \equiv \frac{(2|\mathbf{q}|k + q^2)^2 + 4\left(E_{\mathbf{k}}^f\right)^2 q_4^2}{(2|\mathbf{q}|k - q^2)^2 + 4\left(E_{\mathbf{k}}^f\right)^2 q_4^2}, \quad \beta_f^E \equiv \frac{4(|\mathbf{q}|k + E_{\mathbf{k}}^f(iq_4))^2 - q^4}{4(|\mathbf{q}|k - E_{\mathbf{k}}^f(iq_4))^2 - q^4}. \quad (34)$$

In the second step, we have gotten rid of the term  $\mathbf{q} \cdot \mathbf{k}$  in the numerator to facilitate the integration over the polar angle between  $\mathbf{q}$  and  $\mathbf{k}$ ; in the last step, we have completed both the integrations over solid angles and summation over  $u$ .

Secondly, according to Ref. [27], the other nonvanishing components of the longitudinal part can be given by  $\Pi_{\rho^0 q(t)}^{4i}(q) = -\frac{q^4 q^i}{\mathbf{q}^2} \Pi_{\rho^0 q(t)}^{44}(q)$  ( $i = 1, 2, 3$ ). The relation can be easily justified for the first term of (32), now we are going to show that it is also true for the second term. If we define the tensor in the numerator of the integrand in the second term of (32) by

$$B^{\mu\nu} \equiv q^2 g^{\mu\nu} - q^\mu q^\nu + \left( \frac{2\mathbf{q} \cdot \mathbf{k} - \mathbf{q}^2}{q_4} g^{4\mu} - 2\mathbf{k}^\mu + \mathbf{q}^\mu \right) \left( \frac{2\mathbf{q} \cdot \mathbf{k} - \mathbf{q}^2}{q_4} g^{4\nu} - 2\mathbf{k}^\nu + \mathbf{q}^\nu \right), \quad (35)$$

it follows that

$$\begin{aligned} B^{44} &= \mathbf{q}^2 + \left( \frac{2\mathbf{q} \cdot \mathbf{k} - \mathbf{q}^2}{q_4} \right)^2, \quad B^{4i} = -q^4 q^i - \left( \frac{2\mathbf{q} \cdot \mathbf{k} - \mathbf{q}^2}{q_4} \right) (2\mathbf{k}^i - \mathbf{q}^i), \\ B^{4i} + \frac{q^4 q^i}{\mathbf{q}^2} B^{44} &= - \left( \frac{2\mathbf{q} \cdot \mathbf{k} - \mathbf{q}^2}{q_4} \right) (2\mathbf{k}^i - \mathbf{q}^i - \frac{2\mathbf{q} \cdot \mathbf{k} - \mathbf{q}^2}{\mathbf{q}^2} q^i) = -2 \left( \frac{2\mathbf{q} \cdot \mathbf{k} - \mathbf{q}^2}{q_4} \right) \left( \mathbf{k}^i - \frac{\mathbf{q} \cdot \mathbf{k}}{\mathbf{q}^2} q^i \right). \end{aligned} \quad (36)$$

Then, apart for the  $\mathbf{k}$ -even term  $\frac{n_f^t(\mathbf{k})}{E_{\mathbf{k}}^f}$ , the left of the integrand can be evaluated alternatively by

$$\frac{1}{2} \left[ \frac{B^{4i} + \frac{q^4 q^i}{\mathbf{q}^2} B^{44}}{2u t E_{\mathbf{k}}^f(iq_4) + 2\mathbf{q} \cdot \mathbf{k} + q^2} + \frac{A^{4i} + \frac{q^4 q^i}{\mathbf{q}^2} A^{44}}{2u t E_{\mathbf{k}}^f(iq_4) + 2\mathbf{q} \cdot \mathbf{k} + q^2} \Big|_{\mathbf{k} \rightarrow -\mathbf{k}} \right] = -4 \frac{(k^i - \frac{\mathbf{q} \cdot \mathbf{k}}{\mathbf{q}^2} q^i) \mathbf{q} \cdot \mathbf{k} (2u t E_{\mathbf{k}}^f(iq_4) - q_4^2)}{(2u t E_{\mathbf{k}}^f(iq_4) + q^2)^2 - (2\mathbf{q} \cdot \mathbf{k})^2} \quad (37)$$

for the integration over  $\mathbf{k}$ . As we can see,  $\mathbf{k} - \frac{\mathbf{q} \cdot \mathbf{k}}{\mathbf{q}^2} \mathbf{q}$  is the component of  $\mathbf{k}$  perpendicular to  $\mathbf{q}$  while  $\mathbf{q} \cdot \mathbf{k}$  is determined by  $\mathbf{k}$  parallel to  $\mathbf{q}$ , we can change the sign of  $\mathbf{k} - \frac{\mathbf{q} \cdot \mathbf{k}}{\mathbf{q}^2} \mathbf{q}$  but keep that of  $\mathbf{q} \cdot \mathbf{k}$  for the integration and the convolution of (37) with  $\frac{n_f^t(\mathbf{k})}{E_{\mathbf{k}}^f}$  must vanish. So, the relation  $\Pi_{\rho^0 q(t)}^{4i}(q) = -\frac{q^4 q^i}{\mathbf{q}^2} \Pi_{\rho^0 q(t)}^{44}(q)$  is indeed satisfied and the Ward Identity  $q_4 \Pi_{\rho^0 q(t)}^{44}(q) + q_i \Pi_{\rho^0 q(t)}^{i4}(q) = 0$  is intact as should be.

Thirdly, turn to the transverse part, it can be reduced as the following,

$$\begin{aligned}
\Pi_{\rho^0 q(t)}^{ij}(q) &= -\frac{3g_{vq}^2}{2}g^{ij} \sum_{f=u,d} \int \frac{d^3\mathbf{k}}{(2\pi)^3} \sum_{t=\pm} \frac{n_f^t(\mathbf{k})}{E_{\mathbf{k}}^f} - \frac{3g_{vq}^2}{4} \sum_{f=u,d} \int \frac{d^3\mathbf{k}}{(2\pi)^3} \sum_{u,t=\pm} \frac{q^2 g^{ij} - q^i q^j + (2\mathbf{k} - \mathbf{q})^i (2\mathbf{k} - \mathbf{q})^j}{[2u t E_{\mathbf{k}}^f(iq_4) + 2\mathbf{q} \cdot \mathbf{k} + q^2]} \frac{n_f^t(\mathbf{k})}{E_{\mathbf{k}}^f} \\
&= -\frac{3g_{vq}^2}{2}g^{ij} \sum_{f=u,d} \int \frac{d^3\mathbf{k}}{(2\pi)^3} \sum_{t=\pm} \frac{n_f^t(\mathbf{k})}{E_{\mathbf{k}}^f} - \frac{3g_{vq}^2}{4} \sum_{f=u,d} \int \frac{d^3\mathbf{k}}{(2\pi)^3} \sum_{u,t=\pm} \frac{q^2 g^{ij} - q^i q^j + 4 \left( \mathbf{k} - \frac{\mathbf{q} \cdot \mathbf{k}}{\mathbf{q}^2} \mathbf{q} \right)^i \left( \mathbf{k} - \frac{\mathbf{q} \cdot \mathbf{k}}{\mathbf{q}^2} \mathbf{q} \right)^j + \left( 1 - 2 \frac{\mathbf{q} \cdot \mathbf{k}}{\mathbf{q}^2} \right)^2 \mathbf{q}^i \mathbf{q}^j}{[2u t E_{\mathbf{k}}^f(iq_4) + 2\mathbf{q} \cdot \mathbf{k} + q^2]} \frac{n_f^t(\mathbf{k})}{E_{\mathbf{k}}^f} \\
&= -\frac{3g_{vq}^2}{2}g^{ij} \sum_{f=u,d} \int \frac{d^3\mathbf{k}}{(2\pi)^3} \sum_{t=\pm} \frac{n_f^t(\mathbf{k})}{E_{\mathbf{k}}^f} - \frac{3g_{vq}^2}{4} \sum_{f=u,d} \int \frac{d^3\mathbf{k}}{(2\pi)^3} \sum_{u,t=\pm} \frac{q^2 g^{ij} - q^i q^j - 4 \left( \mathbf{k} - \frac{\mathbf{q} \cdot \mathbf{k}}{\mathbf{q}^2} \mathbf{q} \right)^2 \left( g^{ij} + \frac{q^i q^j}{\mathbf{q}^2} \right) + \left( 1 - 2 \frac{\mathbf{q} \cdot \mathbf{k}}{\mathbf{q}^2} \right)^2 \mathbf{q}^i \mathbf{q}^j}{[2u t E_{\mathbf{k}}^f(iq_4) + 2\mathbf{q} \cdot \mathbf{k} + q^2]} \frac{n_f^t(\mathbf{k})}{E_{\mathbf{k}}^f} \\
&= -\frac{3g_{vq}^2}{2}g^{ij} \sum_{f=u,d} \int \frac{d^3\mathbf{k}}{(2\pi)^3} \sum_{t=\pm} \frac{n_f^t(\mathbf{k})}{E_{\mathbf{k}}^f} - \frac{3g_{vq}^2}{4} \sum_{f=u,d} \int \frac{d^3\mathbf{k}}{(2\pi)^3} \sum_{u,t=\pm} \frac{\left[ q^2 - 4 \left( \mathbf{k}^2 - \frac{(\mathbf{q} \cdot \mathbf{k})^2}{\mathbf{q}^2} \right) \right] g^{ij} - 4 \left[ \mathbf{k}^2 + \mathbf{q} \cdot \mathbf{k} - 2 \frac{(\mathbf{q} \cdot \mathbf{k})^2}{\mathbf{q}^2} \right] \frac{q^i q^j}{\mathbf{q}^2}}{[2u t E_{\mathbf{k}}^f(iq_4) + 2\mathbf{q} \cdot \mathbf{k} + q^2]} \frac{n_f^t(\mathbf{k})}{E_{\mathbf{k}}^f} \\
&= \frac{3g_{vq}^2 q_4^2}{2 \mathbf{q}^2} \left( g^{ij} + 2 \frac{q^i q^j}{\mathbf{q}^2} \right) \sum_{f=u,d} \int \frac{d^3\mathbf{k}}{(2\pi)^3} \sum_{t=\pm} \frac{n_f^t(\mathbf{k})}{E_{\mathbf{k}}^f} + \frac{3g_{vq}^2}{4} \sum_{f=u,d} \int \frac{d^3\mathbf{k}}{(2\pi)^3} \sum_{u,t=\pm} \frac{1}{[2u t E_{\mathbf{k}}^f(iq_4) + 2\mathbf{q} \cdot \mathbf{k} + q^2]} \frac{n_f^t(\mathbf{k})}{E_{\mathbf{k}}^f} \\
&\quad \times \left\{ \left[ q^2 - 4\mathbf{k}^2 + \frac{(2u t E_{\mathbf{k}}^f(iq_4) + q^2)^2}{\mathbf{q}^2} \right] g^{ij} + 2 \left[ q^2 - 2\mathbf{k}^2 + \frac{(2u t E_{\mathbf{k}}^f(iq_4) + q^2)^2}{\mathbf{q}^2} + 2u t E_{\mathbf{k}}^f(iq_4) \right] \frac{q^i q^j}{\mathbf{q}^2} \right\} \\
&= \frac{3g_{vq}^2 q_4^2}{2 \mathbf{q}^2} \left( g^{ij} + 2 \frac{q^i q^j}{\mathbf{q}^2} \right) \sum_{f=u,d} \int \frac{d^3\mathbf{k}}{(2\pi)^3} \sum_{t=\pm} \frac{n_f^t(\mathbf{k})}{E_{\mathbf{k}}^f} + \frac{3g_{vq}^2}{4} \sum_{f=u,d} \int \frac{d^3\mathbf{k}}{(2\pi)^3} \sum_{u,t=\pm} \frac{1}{[2u t E_{\mathbf{k}}^f(iq_4) + 2\mathbf{q} \cdot \mathbf{k} + q^2]} \frac{n_f^t(\mathbf{k})}{E_{\mathbf{k}}^f} \\
&\quad \times \left\{ \left[ -\frac{q_4^2}{\mathbf{q}^2} \left( 4(E_{\mathbf{k}}^f)^2 + q^2 \right) - 4\mathbf{k}^2 + \frac{q^2}{\mathbf{q}^2} 4u t E_{\mathbf{k}}^f(iq_4) \right] g^{ij} + 2 \left[ -\frac{q_4^2}{\mathbf{q}^2} \left( 4(E_{\mathbf{k}}^f)^2 + q^2 \right) - 2\mathbf{k}^2 + \frac{q^2 - q_4^2}{\mathbf{q}^2} 2u t E_{\mathbf{k}}^f(iq_4) \right] \frac{q^i q^j}{\mathbf{q}^2} \right\} \\
&= \frac{3g_{vq}^2}{8} \sum_{f=u,d} \int \frac{k dk}{(2\pi)^2 |\mathbf{q}|} \sum_{t=\pm} \frac{n_f^t(\mathbf{k})}{E_{\mathbf{k}}^f} \left\{ \frac{q_4^2}{\mathbf{q}^2} 8k |\mathbf{q}| \left( g^{ij} + 2 \frac{q^i q^j}{\mathbf{q}^2} \right) + \left[ \left( -\frac{q_4^2}{\mathbf{q}^2} \left( 4(E_{\mathbf{k}}^f)^2 + q^2 \right) - 4\mathbf{k}^2 \right) \ln \alpha_f + \frac{4q^2}{\mathbf{q}^2} E_{\mathbf{k}}^f(iq_4) \ln \beta_f \right] g^{ij} \right. \\
&\quad \left. + 2 \left[ \left( -\frac{q_4^2}{\mathbf{q}^2} \left( 4(E_{\mathbf{k}}^f)^2 + q^2 \right) - 2\mathbf{k}^2 \right) \ln \alpha_f + 2 \frac{q^2 - q_4^2}{\mathbf{q}^2} E_{\mathbf{k}}^f(iq_4) \ln \beta_f \right] \frac{q^i q^j}{\mathbf{q}^2} \right\}. \tag{38}
\end{aligned}$$

In the third step, we have used the property  $(\mathbf{k} - \frac{\mathbf{q} \cdot \mathbf{k}}{\mathbf{q}^2} \mathbf{q}) \perp \mathbf{q}$  to separate the terms parallel to and perpendicular to  $\mathbf{q}$ . The tensor structure  $(g^{ij} + \frac{q^i q^j}{\mathbf{q}^2})$  is obtained by transforming the coordinates from the momentum-dependent Descartes system with axes along  $\mathbf{q}, \mathbf{q} \times \mathbf{k}, (\mathbf{k} - \frac{\mathbf{q} \cdot \mathbf{k}}{\mathbf{q}^2} \mathbf{q})$  to the momentum-independent system with axes along  $x, y, z$ . Notice that the tensor structure well keeps the symmetry between the indices  $i$  and  $j$  and the following features

$$\mathbf{q}_i \left( \mathbf{k} - \frac{\mathbf{q} \cdot \mathbf{k}}{\mathbf{q}^2} \mathbf{q} \right)^i = 0, \quad \left( \mathbf{k} - \frac{\mathbf{q} \cdot \mathbf{k}}{\mathbf{q}^2} \mathbf{q} \right)_i \left( \mathbf{k} - \frac{\mathbf{q} \cdot \mathbf{k}}{\mathbf{q}^2} \mathbf{q} \right)^i \left( \mathbf{k} - \frac{\mathbf{q} \cdot \mathbf{k}}{\mathbf{q}^2} \mathbf{q} \right)^j = - \left( \mathbf{k} - \frac{\mathbf{q} \cdot \mathbf{k}}{\mathbf{q}^2} \mathbf{q} \right)^2 \left( \mathbf{k} - \frac{\mathbf{q} \cdot \mathbf{k}}{\mathbf{q}^2} \mathbf{q} \right)^j. \tag{39}$$

Similar to the derivations in (34), we have gotten rid of the term  $\mathbf{q} \cdot \mathbf{k}$  in the numerator in the fifth step and completed both the integrations over solid angles and summation over  $u$  in the last step. Again, one can check that the Ward Identity  $q_4 \Pi_{\rho^0 q(t)}^{4j}(q) + q_i \Pi_{\rho^0 q(t)}^{ij}(q) = 0$  is intact as should be for the spatial part with  $j = 1, 2, 3$ .

Eventually, the contributions of the thermal part to the self-energies of longitudinal and transverse polarized  $\rho^0$  mesons can be derived and given in Minkowski space as

$$F_q^t = \frac{3g_{vq}^2 M^2}{8 \mathbf{q}^2} \sum_{f=u,d}^{t=\pm} \int \frac{k dk}{(2\pi)^2 |\mathbf{q}|} \frac{n_f^t(\mathbf{k})}{E_{\mathbf{k}}^f} \left[ -8|\mathbf{q}| k + \left( 4 \left( E_{\mathbf{k}}^f \right)^2 + M^2 \right) (\ln |\alpha_f| - i\pi\Delta_f) + 4E_{\mathbf{k}}^f E (\ln |\beta_f| + i\pi\Delta_f) \right], \tag{40}$$

$$G_q^t = \frac{3g_{vq}^2 E^2}{8 \mathbf{q}^2} \sum_{f=u,d}^{t=\pm} \int \frac{k dk}{(2\pi)^2 |\mathbf{q}|} \frac{n_f^t(\mathbf{k})}{E_{\mathbf{k}}^f} \left[ 8k |\mathbf{q}| - \left( 4(E_{\mathbf{k}}^f)^2 + M^2 - 4 \frac{|\mathbf{q}|^2 k^2}{E^2} \right) (\ln |\alpha_f| - i\pi\Delta_f) - 4 \frac{E_{\mathbf{k}}^f}{E} M^2 (\ln |\beta_f| + i\pi\Delta_f) \right]. \tag{41}$$

with the auxiliary functions

$$\alpha_f \equiv \frac{(M^2 + 2k|\mathbf{q}|)^2 - 4(E_{\mathbf{k}}^f)^2 E^2}{(M^2 - 2k|\mathbf{q}|)^2 - 4(E_{\mathbf{k}}^f)^2 E^2}, \quad \beta_f \equiv \frac{M^4 - 4(k|\mathbf{q}| + E_{\mathbf{k}}^f E)^2}{M^4 - 4(k|\mathbf{q}| - E_{\mathbf{k}}^f E)^2}, \quad (42)$$

$$\Delta_f = \text{Boole}(\left|E\sqrt{1-4\tilde{m}_f^2} - |\mathbf{q}|\right| \leq 2k \leq E\sqrt{1-4\tilde{m}_f^2} + |\mathbf{q}|). \quad (43)$$

The main structures of  $F_{\mathbf{q}}^t$  and  $G_{\mathbf{q}}^t$  are similar to those of  $F_{\pi}^t$  in (22) and  $G_{\pi}^t$  in (23) and can be rendered the same by taking the substitutions,  $E^2 \rightarrow M^2$  (thus  $M^2 \rightarrow E^2 - 2|\mathbf{q}|^2$ ) in the nonlogarithmic terms and  $M^4 \rightarrow E^2 M^2$  in front of  $\ln |\alpha_{\pi}|$ .